PHYSICAL REVIEW B **92**, 201108(R) (2015)

Anomalous charge and negative-charge-transfer insulating state in cuprate chain compound $KCuO_2$

D. Choudhury,[1,2,*] P. Rivero,[1] D. Meyers,[1] X. Liu,[1] Y. Cao,[1] S. Middey,[1] M. J. Whitaker,[3] S. Barraza-Lopez,[1] J. W. Freeland,[4] M. Greenblatt,[3] and J. Chakhalian[1]

[1]*Department of Physics, University of Arkansas, Fayetteville, Arkansas 72701, USA*

[2]*Department of Physics, Indian Institute of Technology Kharagpur, Kharagpur 721302, India*

[3]*Department of Chemistry and Chemical Biology, Rutgers University, Piscataway, New Jersey 08854-8087, USA*

[4]*Advanced Photon Source, Argonne National Laboratory, Argonne, Illinois 60439, USA*

(Received 22 April 2015; revised manuscript received 3 November 2015; published 19 November 2015)

Using a combination of x-ray absorption spectroscopy (XAS) experiments and first-principles calculations, we demonstrate that insulating $KCuO_2$ contains Cu in an unusually high formal 3+ valence state, and the ligand-to-metal (O-to-Cu) charge-transfer energy is intriguingly negative ($\Delta \sim -1.5$ eV) and has a dominant ($\sim$60%) ligand-hole character in the ground state akin to the high T_c cuprate Zhang-Rice state. Unlike most other formal Cu^{3+} compounds, the Cu $2p$ XAS spectra of $KCuO_2$ exhibit pronounced $3d^8$ (Cu^{3+}) multiplet structures, which account for $\sim$40% of its ground state wave function. *Ab initio* calculations elucidate the origin of the band gap in $KCuO_2$ as arising primarily from strong intracluster Cu $3d$-O $2p$ hybridizations (t_{pd}); the value of the band gap decreases with a reduced value of t_{pd}. Further, unlike conventional negative-charge-transfer insulators, the band gap in $KCuO_2$ persists even for vanishing values of Coulomb repulsion U, underscoring the importance of single-particle band-structure effects connected to the one-dimensional nature of the compound.

DOI: 10.1103/PhysRevB.92.201108 PACS number(s): 71.30.+h, 78.70.Dm, 71.27.+a, 71.15.Mb

The electronic properties of strongly correlated transition metal (TM) oxides—which consist of partially filled TM d orbitals hybridized with the ligand (oxygen) p orbitals—are effectively categorized under the well known Zaanen-Sawatzky-Allen (ZSA) phase diagram [1–3], a guiding principle for materials scientists that takes into consideration the on-site d-d Coulomb interaction energy at the TM site (U) and the ligand-to-TM charge-transfer energy (Δ). There is an intriguing region of the ZSA phase diagram of compounds with negative values of Δ that has been less explored [4–10]. In TM oxides, the value of Δ decreases by increasing the valence (oxidation) state of the TM ion, and for unusually high-valence states, Δ can even become negative [8]. Such high-valence compounds are very unstable, and only a few pristine negative Δ compounds exist (see Table I). For such highly covalent compounds, it is energetically favorable to transfer an electron from the ligand to the metal ion, as the energy cost Δ for this process is negative, giving rise to a large *ligand-hole* character and a usually metallic nature of the ground state. However, there exist a very select number of compounds, which are insulating while having negative or extremely small values of Δ, driven by a combination of strong metal-ligand hybridization either with strong electronic correlations, as in the case of the correlated covalent insulators [4,6,15,16], as in Sr_2CuO_3 [17], or describable within an effective single-particle band structure, as in the case of $NaCuO_2$ [5,7,8,15,18,19].

In this Rapid Communication, using x-ray absorption spectroscopy (XAS) experiments, model XAS, and density functional theory (DFT) calculations, we have investigated the electronic structure of $KCuO_2$ [20], and have elucidated the nature of its experimentally observed insulating state. Our results suggest that $KCuO_2$ hosts Cu in a formal 3+ valence state, and has a negative Δ and a dominant ligand-hole character on its ground state. We find a charge band gap ($\sim$1.24 eV) with a preponderance of O $2p$ states at the valence band and conduction band edges, which originates from strong intracluster Cu $3d$-O $2p$ hybridization in this negative Δ compound and competes with point-charge Coulomb contributions to the crystal-field energies of the Cu t_{2g} orbitals. The chain-topology driven band gap persists for vanishing U, which is distinct from the conventional picture of correlated covalent insulators [4,6,15], and also decreases with decreasing values of t_{pd}. The inclusion of additional electron-electron correlations with the use of a non-negligible value of U is, however, necessary to account for the experimental value of the gap. Our work thus establishes that $KCuO_2$, similar to $NaCuO_2$, is a negative Δ insulator where the insulating behavior arises from single-particle band-structure effects from the unique one-dimensional CuO_2 chain geometry and electron-electron correlations accounted for within an effective U term.

Methods (experiment). Single-phase polycrystalline $KCuO_2$ was synthesized in an orthorhombic *Cmcm* space group by mixing KO_2 and CuO powders in a 1:1 ratio in an Ar-filled glove box, followed by sintering under a dry O_2 atmosphere for 2.5 days at 450 °C [21]. XA measurements at the Cu $L_{2,3}$ and OK edges were performed on the 4-ID-C beam line of the Advanced Photon Source (APS) at Argonne National Laboratory, USA. The sample powder was mounted on the holder using carbon tape under a nitrogen gas atmosphere to ensure minimum exposure to air, and XAS measurements in total-electron-yield (TEY), total-fluorescence-yield (TFY), and in the inverse-partial-fluorescence-yield (IPFY) modes were performed at room temperature without any additional surface preparation. The probing depth in the case of the TEY ($\sim$5 nm) is much smaller than that of TFY or IPFY ($\sim$100 nm) [22], and thus, while TEY studies the undercoordinated surface electronic structure of a solid, the TFY and IPFY are well suited to

*debraj@phy.iitkgp.ernet.in

TABLE I. Coulomb repulsion U and charge-transfer Δ energies (in units of eV) for some transition metal oxides with unusually high formal-valence states for the B site (Fe, Co, Ni, Cu) cation.

Compound	Formal valence	U	Δ	Transport	Ref.
$SrFeO_3$	(4+)	7.8	0.0	Metal	[2]
$BaFeO_3$	(4+)	7.1	−0.9	Insulator	[11]
$SrCoO_3$	(4+)	7.0	−5.0	Metal	[12]
$LaNiO_3$	(3+)	7.0	1.0	Metal	[13]
$LaCuO_3$	(3+)	7.0	−1.0	Metal	[14]
$NaCuO_2$	(3+)	8.0	−2.5	Insulator	[7]
$KCuO_2$	(3+)	8.0	−1.5	Insulator	This work

investigate the bulk electronic structure. The nonresonant O K edge was monitored during IPFY measurements: These IPFY measurements are further free from any self-absorption effects that may still be present in the TFY spectra [23].

Methods (theory). We have performed three sets of complementary calculations. To act as reference XAS spectra, calculations of the Cu $L_{2,3}$ XA spectrum on a orthorhombic *Cmcm* space-group lattice of $KCuO_2$ [24] [e.g., Fig. 1(a)] were performed using the finite difference method near-edge structure (FDMNES) code [25]. The FDMNES calculations were performed using the full-multiple-scattering theory with a cluster radius of 6 Å around the absorbing Cu atom and an on-site Coulomb energy (U) of 8 eV.

In order to determine the relative TM-O covalencies, cluster calculations for simulating the Cu $L_{2,3}$ XA spectrum of a single CuO_2 planar cluster with a D_{4h} symmetry [26] were performed using the charge-transfer multiplet program for x-ray absorption spectroscopy (CTM4XAS) [27]. The charge-transfer energy Δ between Cu $3d$ and O $2p$ orbitals is defined as $E(d^{n+1}\underline{L}) - E(d^n)$, where $E(d^n)$ is the multiplet-averaged energy for n-electron occupancy on Cu $3d$ levels and $E(d^{n+1}\underline{L})$ denotes the multiplet-averaged energy obtained after transferring one electron from an O $2p$ level to the Cu $3d$ level having $n = 8$ electrons, corresponding to the formal (3+) valence state of Cu. For the CTM4XAS calculations, the basis size was restricted up to one electron charge transfer from O $2p$ to Cu $3d$.

To determine the density of states (DOS) of $KCuO_2$ and $NaCuO_2$, the rotationally invariant local density approximation (LDA+U) scheme of Dudarev *et al.* [28] was employed in DFT electronic structure calculations. Calculations were carried out with the Vienna *ab initio* simulation package (VASP) [29] using projector augmented-wave pseudopotentials [30,31]. The first Brillouin zone was sampled using a 12 × 12 × 6 Monkhorst-Pack set of k points and a 400 eV energy cutoff.

Results and discussion. Two distinct groups of experimentally observed XAS peaks, one around 930 eV (L_3 region) and another group around 950 eV (L_2 region), can be clearly identified for the Cu $L_{2,3}$ edge of $KCuO_2$ [cf. Fig. 1(c)]. While the spectral features for the L_3 and L_2 regions are nearly identical, they are separated by about 20 eV due to the 3/2 × Cu $2p$ core-spin-orbit coupling. Looking around the Cu L_3 region closely, we observe two intense peaks at 930.3 and 932.3 eV, which correspond to the Cu d^9 and the Cu $d^9\underline{L}$ initial states, respectively [32–34].

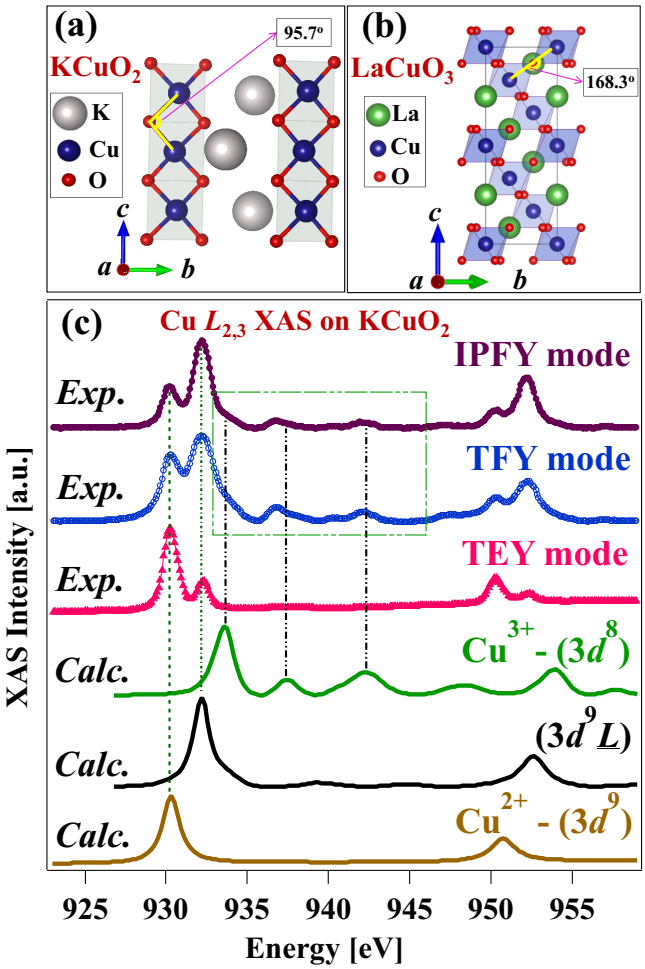

FIG. 1. (Color online) Schematic crystal structures showing (a) edge sharing of CuO_4 units in $KCuO_2$ and (b) corner sharing of CuO_6 clusters for $LaCuO_3$. (c) Cu $L_{2,3}$ x-ray absorption (XA) spectra of $KCuO_2$ collected in the inverse-partial-fluorescence-yield (IPFY), the total-fluorescence-yield (TFY), and the total-electron-yield (TEY) modes. Calculated XA spectra (solid lines) of $KCuO_2$ with the FDMNES code for $3d^9$, $3d^8$, and $3d^9\underline{L}$ configurations are also shown.

The d^9 (Cu^{2+}) peak intensity increases significantly in the TEY mode as compared to the TFY and IPFY modes, indicating an abundance of Cu^{2+} valence states on the surface (see the *Methods* section). This Cu^{2+} presence is believed to arise due to the presence of surface impurity phases rich in Cu^{2+}. Note that similar peaks of d^9 (Cu^{2+}) have been observed for other formal Cu^{3+} compounds in the XA spectrum (e.g., $NaCuO_2$ [5,8,32], $CaCu_3Co_4O_{12}$ [34], and Cs_2KCuF_6 [35]). Cu^{2+} impurity phases on the surfaces of these metastable compounds arise due to the loss of superficial anionic atoms during XAS experiments in ultrahigh vacuum, which effectively reduces the valence of surrounding Cu ions [8]. Further, we observed that $KCuO_2$ on exposure to air decomposes into CuO within 5–10 min. Thus, given these constraints, it is impossible for us to avoid the Cu^{2+} related impurity peak in the XAS experiments. Within the bulk, $KCuO_2$ is not expected to suffer from such anionic losses and, accordingly, much lower intensity Cu^{2+} peaks in the bulk-sensitive TFY and IPFY XAS spectra are observed in Fig. 1(c). Some percentages

of the TFY and IPFY signals are also contributed from the surface and near-surface regions of the sample, which is dominant due to the powder nature of the $KCuO_2$ sample as compared to a scraped bulk-polycrystalline pellet of $NaCuO_2$ [32], that still provides significant contributions of the d^9 peak. The differences in the relative spectral weights among IPFY and TFY data [36] are assigned to known self-absorption effects [23] on the TFY spectra.

Focusing henceforth on the IPFY spectrum, as it is both bulk sensitive and free from self-absorption effects, the main peak given by the $d^9\underline{L}$ state arises due to the charge transfer of an electron from the surrounding O atoms into a formal Cu $3d^8$ (Cu^{3+}) state [32–34]. Furthermore, distinct multiplet structures—that are considered to provide clear evidence for the presence of an ionic Cu^{3+} (d^8) state [32–34]—are observed around 940 eV. The presence of significant $d^9\underline{L}$ and d^8 intensities suggests that a coherent superposition of both states constitutes the ground state of formal Cu^{3+} ions in $KCuO_2$, similar to that of $NaCuO_2$ [32]. It is important to note that on a Cu $2p$-$3d$ XAS process it is difficult to detect contributions from the $d^{10}\underline{L}^2$ level to the ground state. However, such contributions are usually small, as determined by x-ray photoelectron spectroscopy on related systems [8].

To further establish the origin of the various features in the experimental XAS spectra, we simulated the Cu $L_{2,3}$ XAS spectra of $KCuO_2$ that correspond to the d^8, d^9, and $d^9\underline{L}$ initial state configurations using the FDMNES code. As shown by the vertical guidelines in Fig. 1(c), the calculated XAS spectra correspond to the d^9 and $d^9\underline{L}$ features in the experimental spectra, and the observed ionic d^8 experimental features can be broadly understood with the calculated spectrum for the d^8 ionic Cu^{3+} state.

We now compare the L_3 energy region for $KCuO_2$ with other systems that host unusual valence states of Cu, such as the optimally doped $YBa_2Cu_3O_{7-\delta}$ (YBCO) [34], $LaCuO_3$ [34], and $NaCuO_2$ [32] in Fig. 2(a), after subtraction of the surface Cu^{2+} impurity peak [37,38]. It is interesting to note that the Zhang-Rice spin-singlet state $d^9\underline{L}$ [39,40], which arises due to external hole doping in YBCO by chemical routes [32], naturally becomes the dominant state in formal Cu^{3+} compounds. This hole-doping mechanism is akin to a self-doping effect [41]. Judging from the intensity ratios shown in Fig. 2, the $d^9\underline{L}$ charge-transfer state appears dominant over the ionic d^8 state for $KCuO_2$, $NaCuO_2$, and $LaCuO_3$, thus suggesting that the associated charge-transfer energies Δ for all of these compounds are unusually *negative*. We note that negative values of Δ have been proposed already for insulating $NaCuO_2$ [5,7,8] and metallic $LaCuO_3$ [14].

A closer analysis of the XA shapes in Fig. 2(a) points to spectral differences within several formal Cu^{3+} compounds. Let us focus first on the differences in the XA spectral features related to the $d^9\underline{L}$ state: The $d^9\underline{L}$ peak for $LaCuO_3$ is broad and can be well described using two peaks, one centered at 930.8 eV and another at 932.2 eV. This splitting occurs from the delocalization of the ligand hole, due to intercluster hybridization effects that are aided by the corner-sharing geometry of the CuO_6 clusters with a Cu-O-Cu bond angle of 168.3° in $LaCuO_3$ [14] [cf. Fig. 1(b)]. For $KCuO_2$ and $NaCuO_2$, on the other hand, such intercluster hybridization effects are negligible due to the near-orthogonal Cu-O-Cu bond angle (95.7°) between neighboring CuO_4 clusters [cf. Fig. 1(a)] and a single $d^9\underline{L}$ peak is observed.

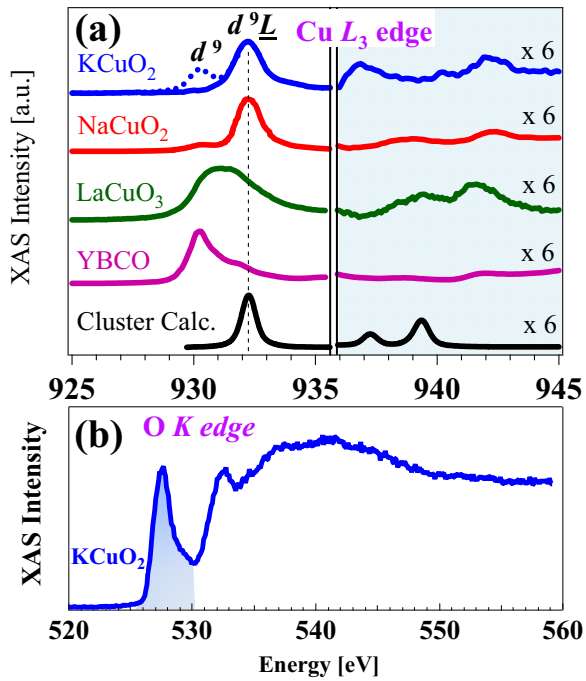

FIG. 2. (Color online) (a) Cu L_3 x-ray absorption (XA) spectra of $KCuO_2$, $NaCuO_2$ [32], $LaCuO_3$, and $YBa_2Cu_3O_{7-\delta}$ (YBCO). The main Cu L_3 peak in $KCuO_2$ and $NaCuO_2$, and the shoulder in YBCO around 932 eV, correspond to the d^9 $\underline{L}$ Zhang-Rice singlet state. The d^8 multiplet structures, sixfold increased for easier observation, are also shown. The calculated XAS spectrum for a single undistorted CuO_4 cluster of D_{4h} symmetry and corresponding to $\Delta = -1.5$ eV is also shown. (b) The O K-edge XA spectrum of $KCuO_2$ consists of a pronounced prepeak around 527.6 eV (shaded area), suggesting a large ligand-hole character of its ground state.

The d^8 multiplet region of formal Cu^{3+} compounds shown by the shaded area in Fig. 2(a) is discussed next. Covalency and Δ are not independent, since the relative intensities between the d^8 multiplets to the $d^9\underline{L}$ peak usually increase with decreasing covalency, and their energy separation increases with larger negative values of Δ [35]. $KCuO_2$ has stronger multiplet intensities than isostructural $NaCuO_2$, which suggests a larger contribution of the ionic d^8 state to its ground state. Further, the average energy difference between the d^8 multiplets and the $d^9\underline{L}$ peak is 5.9 and 8.2 eV for $KCuO_2$ and $NaCuO_2$, respectively, thus showing a smaller negative Δ for $KCuO_2$.

For the calculated Cu $L_{2,3}$ XA spectra on a single CuO_4 cluster with planar D_{4h} symmetry [42], we optimized the parameter values to match the calculated energy separations between the average d^8 multiplets and the $d^9\underline{L}$ main peak with energy differences obtained from experiment [Fig. 2(a)]. The estimated Δ, thus obtained, turned out to be -1.5 and -2.5 eV for $KCuO_2$ and $NaCuO_2$, respectively. Furthermore, both the resultant ground states have dominant $d^9\underline{L}$ characters, $39\%d^8 + 61\%d^9\underline{L}$ ($36\%d^8 + 64\%d^9\underline{L}$) for $KCuO_2$ ($NaCuO_2$), with a higher ionic character for the ground state of $KCuO_2$, as suggested earlier.

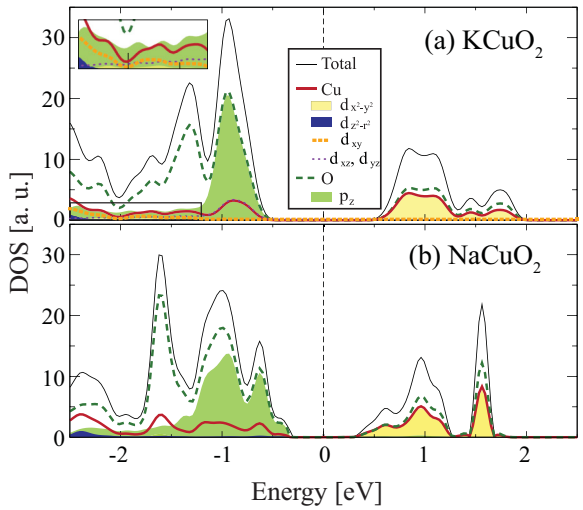

FIG. 3. (Color online) Density of states for (a) $KCuO_2$ and (b) $NaCuO_2$; the total contributions from a given atomic species are indicated by trend lines and the orbital projections are shown by colored area plots. A U of 8 eV was used for these calculations. $KCuO_2$ is found to exhibit a larger band gap than $NaCuO_2$.

The O K-edge XA spectrum—which probes the ligand-hole states—exhibits a pronounced prepeak for $KCuO_2$ at 527.6 eV, as seen in Fig. 2(b). The intensity of the O K-edge prepeak correlates directly with the amount of ligand-hole character in the ground state [35], thus the strong prepeak in $KCuO_2$ further establishes a large $d^9\underline{L}$ character of its ground state.

Figure 3 shows the density of states (DOS) projected onto orbital contributions for $KCuO_2$ and $NaCuO_2$, which were found to have insulating gaps of 1.24 and 0.62 eV, respectively, for the U value of 8 eV. The band gaps in $KCuO_2$ and $NaCuO_2$, however, exist even for $U = 0$ eV, in agreement with previous observations on $NaCuO_2$ [7,15,18], highlighting the role of single-particle band-structure effects due to the chain topology in giving rise to the insulating state in $KCuO_2$. The inclusion of correlations, however, is essential in increasing the band-gap value as compared to $U = 0$ eV and bringing it to the agreement with the experimental value [8]. Furthermore, the projected DOS shows a strong O character in both the valence and conduction band edges [43]. The Cu t_{2g} levels occur between the lower-lying $3d_{3z^2-r^2}$ and higher-lying $3d_{x^2-y^2}$ levels, as usually observed for one-dimensional CuO_2 chains due to point-charge (Coulomb) contributions [44]. However, the t_{2g} levels are intriguingly seen to have Cu (d_{xz}) and Cu (d_{yz}) character immediately below E_F and Cu d_{xy} character only at further lower energies, which is different from a point-charge (Coulomb) contribution to crystal-field splitting. A similar effect has been observed in $Cs_2Au_2Cl_6$, and arises from a dominant pd covalency contribution in the case of negative Δ compounds [10]; the inversion of the t_{2g} orbitals thus further confirms the negative Δ in $KCuO_2$.

We also performed a Bader analysis [45] to understand the charge density distribution over electronic orbitals. The total occupation of the Cu $3d$ shell in both systems is 8.8, which represents a mixture of d^8 and d^9 states, in qualitative agreement with cluster calculations and establishing the superposition of both contributions to the ground state of formal Cu^{3+} ions in $KCuO_2$ and $NaCuO_2$, as discussed earlier.

Conclusions. We have described the presence of the anomalous charge state of Cu in $KCuO_2$ from experiment and theory. We established the negative-charge-transfer energy of the $KCuO_2$ ground state and its dominant ligand-hole character, which arise due to large intracluster hybridization effects and remain localized due to weak intercluster hybridizations. Localized cupratelike Zhang-Rice singlet states thus occur at every unit cell, which consequently give rise to the experimentally observed insulating and diamagnetic character of $KCuO_2$ [20,41]. Moreover, $KCuO_2$ exhibits strong d^8 related multiplet structures, resulting from the large ionic Cu^{3+} character of its ground state. $KCuO_2$ is shown to belong to the unusual class of covalency driven negative-charge transfer insulators with the correlated gap that is adiabatically connected to the single-particle gap arising from the chain geometry of the compound.

Acknowledgments. We deeply thank D. D. Sarma and D. I. Khomskii for insightful suggestions and comments. We thank NSF-XSEDE (Grant No. TG-PHY090002; TACC's *Stampede*) and HPC at Arkansas for computational support. J.C. was funded by the Gordon and Betty Moore Foundation's EPiQS Initiative through Grant No. GBMF4534. S.M. and D.M. were funded by the DOD-ARO under Grant No. 0402-17291 for the synchrotron work at APS. Work at the Advanced Photon Source is supported by the U.S. Department of Energy, Office of Science under Grant No. DEAC02-06CH11357. P.R. and S.B.L. acknowledge funding from the Arkansas Biosciences Institute.

[1] J. Zaanen, G. A. Sawatzky, and J. W. Allen, Phys. Rev. Lett. **55**, 418 (1985).

[2] A. E. Bocquet, T. Mizokawa, T. Saitoh, H. Namatame, and A. Fujimori, Phys. Rev. B **46**, 3771 (1992).

[3] A. E. Bocquet, T. Mizokawa, K. Morikawa, A. Fujimori, S. R. Barman, K. Maiti, D. D. Sarma, Y. Tokura, and M. Onoda, Phys. Rev. B **53**, 1161 (1996).

[4] D. D. Sarma, J. Solid State Chem. **88**, 45 (1990).

[5] T. Mizokawa, H. Namatame, A. Fujimori, K. Akeyama, H. Kondoh, H. Kuroda, and N. Kosugi, Phys. Rev. Lett. **67**, 1638 (1991).

[6] D. D. Sarma, H. R. Krishnamurthy, S. Nimkar, S. Ramasesha, P. P. Mitra, and T. V. Ramakrishnan, Pramana **38**, L531 (1992).

[7] S. Nimkar, D. D. Sarma, and H. R. Krishnamurthy, Phys. Rev. B **47**, 10927 (1993).

[8] T. Mizokawa, A. Fujimori, H. Namatame, K. Akeyama, and N. Kosugi, Phys. Rev. B **49**, 7193 (1994).

[9] M. Imada, A. Fujimori, and Y. Tokura, Rev. Mod. Phys. **70**, 1039 (1998).

[10] A. V. Ushakov, S. V. Streltsov, and D. I. Khomskii, J. Phys.: Condens. Matter **23**, 445601 (2011).

[11] T. Tsuyama, T. Matsuda, S. Chakraverty, J. Okamoto, E. Ikenaga, A. Tanaka, T. Mizokawa, H. Y. Hwang, Y. Tokura, and H. Wadati, Phys. Rev. B **91**, 115101 (2015).
[12] R. H. Potze, G. A. Sawatzky, and M. Abbate, Phys. Rev. B **51**, 11501 (1995).
[13] M. Abbate, G. Zampieri, F. Prado, A. Caneiro, J. M. Gonzalez-Calbet, and M. Vallet-Regi, Phys. Rev. B **65**, 155101 (2002).
[14] T. Mizokawa, T. Konishi, A. Fujimori, Z. Hiroi, M. Takano, and Y. Takeda, J. Electron. Spectrosc. Relat. Phenom. **92**, 97 (1998).
[15] S. Nimkar, N. Shanthi, and D. D. Sarma, Proc. - Indian Acad. Sci., Chem. Sci. **106**, 393 (1994).
[16] D. D. Sarma and A. Taraphder, Phys. Rev. B **39**, 11570 (1989).
[17] K. Maiti, D. D. Sarma, T. Mizokawa, and A. Fujimori, Europhys. Lett. **37**, 359 (1997).
[18] D. J. Singh, Phys. Rev. B **49**, 1580 (1994).
[19] D. I. Khomskii, Lith. J. Phys. **37**, 65 (1997).
[20] G. A. Costa and E. Kaiser, Thermochim. Acta **269/270**, 591 (1995).
[21] See Supplemental Material at http://link.aps.org/supplemental/10.1103/PhysRevB.92.201108 for powder x-ray diffraction data analysis and unit-cell parameters.
[22] S. B. Ogale, T. V. Venkatesan, and M. Blamire, *Functional Metal Oxides: New Science and Novel Applications* (Wiley-VCH, Weinheim, 2013).
[23] A. J. Achkar, T. Z. Regier, E. J. Monkman, K. M. Shen, and D. G. Hawthorn, Sci. Rep. **1**, 182 (2011).
[24] K. Hestermann and R. Hoppe, Z. Anorg. Allg. Chem. **367**, 249 (1969).
[25] O. Bunau and Y. Joly, J. Phys.: Condens. Matter **21**, 345501 (2009).
[26] Such single-cluster model XA calculations apply reasonably well in the case of insulating compounds, especially $KCuO_2$ and $NaCuO_2$, where intercluster hybridization effects can be neglected.
[27] E. Stavitski and F. M. F. de Groot, Micron **41**, 687 (2010).
[28] S. L. Dudarev, G. A. Botton, S. Y. Savrasov, C. J. Humphreys, and A. P. Sutton, Phys. Rev. B **57**, 1505 (1998).
[29] G. Kresse and J. Furthmuller, Phys. Rev. B **54**, 11169 (1996).
[30] P. E. Blöchl, Phys. Rev. B **50**, 17953 (1994).
[31] G. Kresse and D. Joubert, Phys. Rev. B **59**, 1758 (1999).
[32] D. D. Sarma, O. Strebel, C. T. Simmons, U. Neukirch, G. Kaindl, R. Hoppe, and H. P. Muller, Phys. Rev. B **37**, 9784 (1988).
[33] R. Sarangi, N. Aboelella, K. Fujisawa, W. B. Tolman, B. Hedman, K. O. Hodgson, and E. I. Solomon, J. Am. Chem. Soc. **128**, 8286 (2006).
[34] D. Meyers, S. Mukherjee, J. G. Cheng, S. Middey, J. S. Zhou, J. B. Goodenough, B. A. Gray, J. W. Freeland, T. S. Dasgupta, and J. Chakhalian, Sci. Rep. **3**, 1834 (2013).
[35] Z. Hu, G. Kaindl, S. A. Warda, D. Reinen, F. M. F. de Groot, and B. G. Müller, Chem. Phys. **232**, 63 (1998).
[36] The d^9 peak in the TFY spectra does not suffer from self-absorption effects as the impurity phases containing Cu^{2+} ions lie only over the sample surfaces. However, self-absorption effects affect the $d^9\underline{L}$ TFY peak intensity, since it arises from formal Cu^{3+} ions present in high concentrations and spread over the bulk of the sample.
[37] An arc-tangent background function was subtracted from the spectra first, followed by a multipeak-fitting analysis of the L_3 edge; the peak corresponding to Cu^{2+} [shown with the dashed line in Fig. 2(a)] was subtracted subsequently.
[38] The XA spectrum of $NaCuO_2$ in Fig. 2(a) is taken from Ref. [32].
[39] H. Eskes and G. A. Sawatzky, Phys. Rev. Lett. **61**, 1415 (1988).
[40] F. C. Zhang and T. M. Rice, Phys. Rev. B **37**, 3759 (1988).
[41] D. I. Khomskii, *Transition Metal Compounds* (Cambridge University Press, Cambridge, UK, 2014).
[42] D_{4h} effective ligand field parameters: $10D_q = 2.5$ eV, $D_t = 0.24$ eV, $D_s = 0.19$ eV; Coulomb correlations $U_{dd} = 8.0$ eV and $U_{pd} = 10.5$ eV were used. The metal-ligand mixing interaction (T_{B1g}) optimized to -2.42 and -3.46 eV was used for $KCuO_2$ and $NaCuO_2$, respectively.
[43] Due to the extended nature of the O p orbitals, the decomposition of the total DOS by projecting on the linearized augmented plane-wave (LAPW) spheres is known to underestimate the O p character [18], thus the valence and conduction bands have a larger O p character than those obtained under the LDA+U scheme.
[44] M. M. Sala, V. Bisogni, C. Aruta, G. Balestrino, H. Berger, N. B. Brookes, G. M. de Luca, D. D. Castro, M. Grioni, M. Guarise, P. G. Medaglia, F. M. Granozio, M. Minola, P. Perna, M. Radovic, M. Salluzzo, T. Schmitt, K. J. Zhou, L. Braicovich, and G. Ghiringhelli, New J. Phys. **13**, 043026 (2011).
[45] R. F. W. Bader, *Atoms in Molecules: A Quantum Theory* (Oxford University Press, Oxford, UK, 1990).